

- (462) Yuan, J.; Gao, H.; Ching, C. B. *Toxicol. Lett.* **2011**, *207*, 213.
- (463) Haniu, H.; Matsuda, Y.; Usui, Y.; Aoki, K.; Shimizu, M.; Ogihara, N.; Hara, K.; Okamoto, M.; Takanashi, S.; Ishigaki, N.; Nakamura, K.; Kato, H.; Saito, N. *J. Proteomics* **2011**, *74*, 2703.
- (464) Snyder-Talkington, B. N.; Pacurari, M.; Dong, C.; Leonard, S. S.; Schwegler-Berry, D.; Castranova, V.; Qian, Y.; Guo, N. L. *Toxicol. Sci.* **2013**, *133*, 79.
- (465) Lacerda, L.; Herrero, M. A.; Venner, K.; Bianco, A.; Prato, M.; Kostarelos, K. *Small* **2008**, *4*, 1130.
- (466) Helfenstein, M.; Miragoli, M.; Rohr, S.; Muller, L.; Wick, P.; Mohr, M.; Gehr, P.; Rothen-Rutishauser, B. *Toxicology* **2008**, *253*, 70.
- (467) ISO 10993. Biological Evaluation of Medical Devices. 2000–2012.
- (468) Shi, H.; Magaye, R.; Castranova, V.; Zhao, J. *Part. Fibre Toxicol.* **2013**, *10*, 15.
- (469) Kashuk, K. B.; Haber, E. *Clin. Podiatry* **1984**, *1*, 131.
- (470) Parsons, J. R.; Weiss, A. B.; Schenk, R. S.; Alexander, H.; Pavlisko, F. *Foot Ankle* **1989**, *9*, 179.
- (471) Moreira-Gonzalez, A.; Jackson, I. T.; Miyawaki, T.; DiNick, V.; Yavuzer, R. *Plast. Reconstr. Surg.* **2003**, *111*, 1808.
- (472) Tamimi, F.; Torres, J.; Bassett, D.; Barralet, J.; Cabarcos, E. L. *Biomaterials* **2010**, *31*, 2762.
- (473) Goff, T.; Kanakaris, N. K.; Giannoudis, P. V. *Injury* **2013**, *44*, S86.
- (474) Ciftcioglu, N.; Aho, K. M.; McKay, D. S.; Kajander, E. O. *Lancet* **2007**, *369*, 2078.
- (475) Jacobsen, E.; Tønning, K.; Pedersen, E.; Serup, J.; Nielsen, E. *Chemical Substances in Tattoo Ink. Survey of chemical substances in consumer products no. 116*; Miljøstyrelsen: København, 2012.
- (476) Lehman, J. H.; Terrones, M.; Mansfield, E.; Hurst, K.; Muenier, V. *Carbon* **2011**, *49*, 2581.
- (477) U.S. Department of Health and Human Services Food and Drug Administration Office of the Commissioner. Considering whether an FDA-regulated product involves the application of nanotechnology: guidance for industry. Regulatory Information, 2011.
- (478) ISO/TS 27687: 2008, Nanotechnologies - Terminology and definitions for nano-objects - nanoparticle, nanofibre and nanoplate, 2008.
- (479) Chen, Z.; Mao, R.; Liu, Y. *Curr. Drug Metab.* **2012**, *13*, 1035.
- (480) Mao, H. Y.; Laurent, S.; Chen, W.; Akhavan, O.; Imani, M.; Ashkarran, A. A.; Mahmoudi, M. *Chem. Rev.* **2013**, *113*, 3407.
- (481) Misra, R. D.; Chaudhari, P. M. *J. Biomed. Mater. Res., Part A* **2013**, *101*, S28.
- (482) Ando, K.; Saitoh, A.; Hino, O.; Takahashi, R.; Kimura, M.; Katsuki, M. *Cancer Res.* **1992**, *52*, 978.
- (483) Long, G. G.; Morton, D.; Peters, T.; Short, B.; Skydsgaard, M. *Toxicol. Pathol.* **2010**, *38*, 43.
- (484) Boverhof, D. R.; Chamberlain, M. P.; Elcombe, C. R.; Gonzalez, F. J.; Heflich, R. H.; Hernandez, L. G.; Jacobs, A. C.; Jacobson-Kram, D.; Luijten, M.; Maggi, A.; Manjanatha, M. G.; Benthem, J.; Gollapudi, B. B. *Toxicol. Sci.* **2011**, *121*, 207.
- (485) Urano, K.; Tamaoki, N.; Nomura, T. *Vet. Pathol.* **2012**, *49*, 16.
- (486) Urano, K.; Suzuki, S.; Machida, K.; Sawa, N.; Eguchi, N.; Kikuchi, K.; Fukasawa, K.; Taguchi, F.; Usui, T. *J. Toxicol. Sci.* **2006**, *31*, 407.
- (487) Urano, K.; Suzuki, S.; Machida, K.; Eguchi, N.; Sawa, N.; Kikuchi, K.; Hattori, Y.; Usui, T. *J. Toxicol. Sci.* **2007**, *32*, 367.
- (488) Palazzi, X.; Kergozien-Framery, S. *Exp. Toxicol. Pathol.* **2009**, *61*, 433.
- (489) Madani, S. Y.; Naderi, N.; Dissanayake, O.; Tan, A.; Seifalian, A. M. *Int. J. Nanomed.* **2011**, *6*, 2963.
- (490) Heister, E.; Brunner, E. W.; Dieckmann, G. R.; Jurewicz, I.; Dalton, A. B. *ACS Appl. Mater. Interfaces* **2013**, *5*, 1870.
- (491) Madani, S. Y.; Shabani, F.; Dwek, M. V.; Seifalian, A. M. *Int. J. Nanomed.* **2013**, *8*, 941.
- (492) Tang, S.; Tang, Y.; Zhong, L.; Murat, K.; Asan, G.; Yu, J.; Jian, R.; Wang, C.; Zhou, P. *J. Appl. Toxicol.* **2012**, *32*, 900.
- (493) The Organisation for Economic Cooperation and Development (OECD). Six years of OECD work on the safety of manufactured nanomaterials: Achievements and future opportunities. OECD brochure: Overview, 2012.
- (494) Jia, G.; Wang, H.; Yan, L.; Wang, X.; Pei, R.; Yan, T.; Zhao, Y.; Guo, X. *Environ. Sci. Technol.* **2005**, *39*, 1378.
- (495) Nerl, H. C.; Cheng, C.; Goode, A. E.; Bergin, S. D.; Lich, B.; Gass, M.; Porter, A. E. *Nanomedicine* **2011**, *6*, 849.
- (496) Qu, G.; Bai, Y.; Zhang, Y.; Jia, Q.; Zhang, W.; Yan, B. *Carbon* **2009**, *47*, 2060.
- (497) Buford, M. C.; Hamilton, R. F., Jr.; Holian, A. *Part. Fibre Toxicol.* **2007**, *4*, 6.
- (498) Snyder-Talkington, B. N.; Qian, Y.; Castranova, V.; Guo, N. L. *J. Toxicol. Environ. Health, Part B* **2012**, *15*, 468.
- (499) Donaldson, K. *Nanomedicine* **2006**, *1*, 229.
- (500) Lam, C. W.; James, J. T.; McCluskey, R.; Arepalli, S.; Hunter, R. L. *Crit. Rev. Toxicol.* **2006**, *36*, 189.
- (501) Wang, L.; Castranova, V.; Mishra, A.; Chen, B.; Mercer, R. R.; Schwegler-Berry, D.; Rojanasakul, Y. *Part. Fibre Toxicol.* **2010**, *7*, 31.
- (502) Palomäki, J.; Välimäki, E.; Sund, J.; Vippola, M.; Clausen, P. A.; Jensen, K. A.; Savolainen, K.; Matikainen, S.; Alenius, H. *ACS Nano* **2011**, *5*, 6861.
- (503) Patlolla, A. K.; Berry, A.; Tchounwou, P. B. *Mol. Cell. Biochem.* **2011**, *358*, 189.
- (504) Sanchez, V. C.; Weston, P.; Yan, A.; Hurt, R. H.; Kane, A. B. *Part. Fibre Toxicol.* **2011**, *8*, 17.
- (505) Teeguarden, J. G.; Webb-Robertson, B. J.; Waters, K. M.; Murray, A. R.; Kisin, E. R.; Varnum, S. M.; Jacobs, J. M.; Pounds, J. G.; Zanger, R. C.; Shvedova, A. A. *Toxicol. Sci.* **2011**, *120*, 123.
- (506) Patlolla, A. K.; Berry, A.; May, L.; Tchounwou, P. B. *Int. J. Environ. Res. Public Health* **2012**, *9*, 1649.
- (507) Atkins, G. J.; Haynes, D. R.; Howie, D. W.; Findlay, D. M. *World J. Orthop.* **2011**, *2*, 93.
- (508) Blumenfeld, T. J.; McKellop, H. A.; Schmalzried, T. P.; Billi, F. *J. Arthroplasty* **2011**, *26*, 666e5.
- (509) Furmanski, J.; Kraay, M. J.; Rinnac, C. M. *J. Arthroplasty* **2011**, *26*, 796.
- (510) Goldstein, M. J.; Ast, M. P.; Dimai, F. R. *Orthopedics* **2012**, *35*, e1119.
- (511) Waewsawangwong, W.; Goodman, S. B. *J. Arthroplasty* **2012**, *27*, 323 e1.
- (512) Pruitt, L. A.; Ansari, F.; Kury, M.; Mehdizah, A.; Patten, E. W.; Huddleston, J.; Mickelson, D.; Chang, J.; Hubert, K.; Ries, M. D. *J. Biomed. Mater. Res., Part B* **2013**, *101*, 476.
- (513) Regis, D.; Sandri, A.; Bartolozzi, P. *Orthopedics* **2008**, *31*.
- (514) Lee, Y. K.; Yoo, J. J.; Koo, K. H.; Yoon, K. S.; Kim, H. J. *J. Orthop. Res.* **2011**, *29*, 218.
- (515) Lopes, R.; Philippeau, J. M.; Passuti, N.; Gouin, F. *Clin. Orthop. Relat. Res.* **2012**, *470*, 1705.
- (516) Traina, F.; De Fine, M.; Bordini, B.; Toni, A. *Hip Int.* **2012**, *22*, 607.
- (517) Kawano, S.; Sonohata, M.; Shimazaki, T.; Kitajima, M.; Mawatari, M.; Hotokebuchi, T. *J. Arthroplasty* **2013**.
- (518) Koo, K. H.; Ha, Y. C.; Kim, S. Y.; Yoon, K. S.; Min, B. W.; Kim, S. R. *J. Arthroplasty* **2013**.
- (519) Kulkarni, A. G.; Hee, H. T.; Wong, H. K. *Spine J.* **2007**, *7*, 205.
- (520) Kurtz, S. M.; Devine, J. N. *Biomaterials* **2007**, *28*, 4845.
- (521) Yang, J. J.; Yu, C. H.; Chang, B. S.; Yeom, J. S.; Lee, J. H.; Lee, C. K. *Clin. Orthop. Surg.* **2011**, *3*, 16.
- (522) Le, T. V.; Baaj, A. A.; Dakwar, E.; Burkett, C. J.; Murray, G.; Smith, D. A.; Uribe, J. S. *Spine (Philadelphia)* **2012**, *37*, 1268.
- (523) Olivares-Navarrete, R.; Gittens, R. A.; Schneider, J. M.; Hyzy, S. L.; Haithcock, D. A.; Ullrich, P. F.; Schwartz, Z.; Boyan, B. D. *Spine J.* **2012**, *12*, 265.
- (524) Barz, T.; Lange, J.; Melloh, M.; Staub, L. P.; Merk, H. R.; Kloting, I.; Follak, N. *Spine (Philadelphia)* **2013**, *38*, E263.
- (525) Chen, L.; Hu, J.; Shen, X.; Tong, H. *J. Mater. Sci.: Mater. Med.* **2013**, *24*, 1843.
- (526) Gupta, A.; Woods, M. D.; Illingworth, K. D.; Niemeier, R.; Schafer, I.; Cady, C.; Filip, P.; El-Amin, S. F., III. *J. Orthop. Res.* **2013**, *31*, 1374.

(S27) European Commission. Proposal for a regulation of the european parliament and of the council on medical devices, and amending directive 2001/83/ec, regulation (ec) no 178/2002 and regulation (EC) No 1223/2009. COM 2012, 542 final.

(S28) Vardharajula, S.; Ali, S. Z.; Tiwari, P. M.; Eroğlu, E.; Vig, K.; Dennis, V. A.; Singh, S. R. *Int. J. Nanomed.* **2012**, *7*, 5361.

# Biological responses according to the shape and size of carbon nanotubes in BEAS-2B and MESO-I cells

Hisao Haniu<sup>1,2</sup>  
Naoto Saito<sup>2,3</sup>  
Yoshikazu Matsuda<sup>4</sup>  
Tamotsu Tsukahara<sup>5</sup>  
Yuki Usui<sup>1,6,7</sup>  
Kayo Maruyama<sup>2,3</sup>  
Seiji Takanashi<sup>1</sup>  
Kaoru Aoki<sup>1</sup>  
Shinsuke Kobayashi<sup>1</sup>  
Hiroki Nomura<sup>1</sup>  
Manabu Tanaka<sup>1</sup>  
Masanori Okamoto<sup>1</sup>  
Hiroyuki Kato<sup>1</sup>

<sup>1</sup>Department of Orthopaedic Surgery, Shinshu University School of Medicine, Nagano, Japan; <sup>2</sup>Institute for Biomedical Sciences, Shinshu University, Nagano, Japan; <sup>3</sup>Department of Applied Physical Therapy, Shinshu University School of Health Sciences, Nagano, Japan; <sup>4</sup>Clinical Pharmacology Educational Center, Nihon Pharmaceutical University, Saitama, Japan; <sup>5</sup>Department of Hematology and Immunology, Kanazawa Medical University, Ishikawa, Japan; <sup>6</sup>Research Center for Exotic Nanocarbons, Shinshu University, Nagano, Japan; <sup>7</sup>Aizawa Hospital, Sports Medicine Center, Nagano, Japan

Correspondence: Hisao Haniu  
Institute for Biomedical Sciences,  
Shinshu University, 3-1-1 Asahi,  
Matsumoto, Nagano 390-8621, Japan  
Tel +81 263 37 2659  
Fax +81 263 35 8844  
Email hhanu@shinshu-u.ac.jp

**Abstract:** This study aimed to investigate the influence of the shape and size of multi-walled carbon nanotubes (MWCNTs) and cup-stacked carbon nanotubes (CSCNTs) on biological responses in vitro. Three types of MWCNTs – VGCF<sup>®</sup>-X, VGCF<sup>®</sup>-S, and VGCF<sup>®</sup> (vapor grown carbon fibers; with diameters of 15, 80, and 150 nm, respectively) – and three CSCNTs of different lengths (CS-L, 20–80  $\mu$ m; CS-S, 0.5–20  $\mu$ m; and CS-M, of intermediate length) were tested. Human bronchial epithelial (BEAS-2B) and malignant pleural mesothelioma cells were exposed to the CNTs (1–50  $\mu$ g/mL), and cell viability, permeability, uptake, total reactive oxygen species/superoxide production, and intracellular acidity were measured. CSCNTs were less toxic than MWCNTs in both cell types over a 24-hour exposure period. The cytotoxicity of endocytosed MWCNTs varied according to cell type/size, while that of CSCNTs depended on tube length irrespective of cell type. CNT diameter and length influenced cell aggregation and injury extent. Intracellular acidity increased independently of lysosomal activity along with the number of vacuoles in BEAS-2B cells exposed for 24 hours to either CNT (concentration, 10  $\mu$ g/mL). However, total reactive oxygen species/superoxide generation did not contribute to cytotoxicity. The results demonstrate that CSCNTs could be suitable for biological applications and that CNT shape and size can have differential effects depending on cell type, which can be exploited in the development of highly specialized, biocompatible CNTs.

**Keywords:** multi-walled carbon nanotube, cup-stacked carbon nanotube, cytotoxicity, in vitro, intracellular acidity

## Introduction

Due to their unique physicochemical properties, carbon nanotubes (CNTs) have applications in a wide variety of industries. One major area of application is in the manufacture of biomaterials and devices, which include biosensors and drug and vaccine delivery vehicles.<sup>1,2</sup> CNTs have the advantage of superior mechanical strength, and carbon materials in general are considered inert and therefore biocompatible.<sup>3,4</sup> However, before CNTs can be incorporated into new and existing biomedical devices, their toxicity and biocompatibility need to be thoroughly investigated. Mice injected intraperitoneally with CNTs exhibited toxicological changes similar to those induced by exposure to asbestos,<sup>5,6</sup> and CNTs have been linked to the induction of mesotheliomas.<sup>7,8</sup> Although some in vivo studies have been conducted on the safety of CNT exposure by inhalation or intratracheal administration, their findings have been indeterminate.<sup>9–13</sup> Results from in vitro studies have also been ambiguous, with some studies reporting that CNTs induce cytotoxicity and cytokine production,<sup>14–18</sup> and others showing that no significant biological responses are elicited.<sup>19,20</sup>

Many reasons have been proposed for these contradictory findings. First, CNTs can be single-walled, multi-walled (MWCNTs), as well as cup-stacked (CSCNTs), and can differ in terms of length and diameter as well as physiochemical properties such as shape, agglomeration, surface structure, and carbon defects, any of which can influence the toxicological evaluation.<sup>21–27</sup> Moreover, impurities in CNTs have been shown to induce oxidative stress, resulting in cellular damage.<sup>28,29</sup> Other factors besides the CNT itself, such as experimental conditions, have also been suggested to contribute to a misleading toxicity evaluation.<sup>14,30,31</sup> Two recent studies by our group examined the possible factors contributing to the variable cytotoxicity of CNTs in vitro. In one study, it was found that cytotoxicity differed according to the dispersant that is used.<sup>32</sup> CNTs dispersed with gelatin or 1,2-dipalmitoyl-sn-glycero-3-phosphocholine were endocytosed and induced concentration-dependent cytotoxicity and cytokine secretion, while the same was not observed when carboxymethyl cellulose was used instead. Varying degrees of cytotoxicity were also observed in different cell lines.<sup>33</sup> MWCNTs were endocytosed by, and were toxic to, malignant pleural mesothelioma, bronchial epithelial, and macrophage-like cells, but not neuroblastoma and monoblastic cells. Endocytosed MWCNTs accumulated in the lysosome, causing injury to the membrane. However, endocytosed carbon black, a carbon allotrope, had no cytotoxic effects despite settling in the lysosome. This indicates that the toxicity associated with CNTs, which are internalized due to their nanosize, is not an inherent property of the constituent carbon (which is considered inert), but is actually due to other factors.

In the present study, we investigated whether the physical dimensions and type of CNTs influence cellular response. MWCNTs (Showa Denko KK, Tokyo, Japan) and CSCNTs (GSI Creos, Tokyo, Japan) of various diameters and lengths were tested in two different epithelial cell lines, in which responses were evaluated based on several biological parameters. The findings indicate that the cellular response to CNTs is dependent on multiple factors, which should be considered while developing CNTs that have optimal biocompatibility.

## Materials and methods

### CNT preparation

The properties of the MWCNTs are listed in Table 1, and those of the CSCNTs<sup>34</sup> are listed in Table 2. Three types of MWCNTs – VGCF®-X, VGCF®-S, and VGCF® (vapor grown carbon fibers; with diameters of 15, 80, and 150 nm,

**Table 1** Properties of multi-walled carbon nanotubes (MWCNTs)

MWCNTs	VGCF®	VGCF®-S	VGCF®-X
Length (µm)	8	10	3
Diameter (nm)	150	80	15
Agglomeration size (nm)	1,660±38	1,638±98	4,417±401
Iron content (ppm)	34	1,700	12,000

**Note:** MWCNTs were provided by Showa Denko KK (Tokyo, Japan).  
**Abbreviation:** VGCF, vapor grown carbon fibers.

respectively) – and three CSCNTs of different lengths (CS-L, 20–80 µm; CS-S, 0.5–20 µm; and CS-M, of intermediate length) were tested. The CNTs were sterilized by autoclaving at 121°C for 15 minutes, then dispersed in 0.1% gelatin in phosphate-buffered saline (PBS) and sonicated in a water bath for 30 minutes.

### Cell culture

The BEAS-2B human bronchial epithelial cell line was purchased from the American Type Culture Collection (ATCC), (Manassas, VA, USA). The ACC-MESO-1 human malignant pleural mesothelioma cell line<sup>35</sup> was purchased from RIKEN (Wako, Ibaraki, Japan). BEAS-2B cells were cultured in Ham’s Nutrient Mixture F-12 (Nacalai Tesque) with 10% fetal bovine serum ([FBS] Life Technologies, Carlsbad, CA, USA), and MESO-1 cells were cultured in RPMI1640 supplemented with 10% FBS. Both cell lines were cultured at 37°C in a 5% CO<sub>2</sub> humidified incubator and passaged twice a week. For each study, cells were seeded at a density of 2×10<sup>5</sup> or 5×10<sup>5</sup> cells/mL and adhered for 24 hours.

### alamarBlue® (AB) assay

To assess cell viability upon exposure to CNTs, an AB assay (Life Technologies) was performed according to the manufacturer’s instructions. Cells were incubated for 24 hours at 37°C in culture medium with 1, 10, or 50 µg/mL CNTs in 96-well culture plates. Control cells were cultured in medium containing the dispersant medium (0.001% gelatin). Viable cells metabolized the dye, resulting in an increase in fluorescence by excitation/emission at 550/600 nm, which was recorded by a fluorescence multiplate reader (PowerScan 4; DS Pharma Biomedical,

**Table 2** Properties of cup-stacked carbon nanotubes (CSCNTs)

CSCNTs	CS-L	CS-M <sup>a</sup>	CS-S
Length (µm)	20–80		0.5–20
Diameter (nm)	100	100	100
Agglomeration size (nm)	2,029±79	1,833±201	1,547±15

**Notes:** CSCNTs were provided by GSI Creos (Tokyo, Japan). <sup>a</sup>Blank space denotes that CS-M is between CS-L and CS-S in terms of length.

Osaka, Japan). Cytotoxic activity was calculated as follows:

$$\text{Percent cytotoxicity} = 100 \times \frac{\text{experimental value}}{\text{control value}} \quad (1)$$

Each sample was assayed six times.

### Lactate dehydrogenase (LDH) release assay

To determine plasma membrane permeability of cells exposed to CNTs, cells grown in 24-well plates were incubated for 24 hours at 37°C with or without CNT (10 µg/mL). LDH activity in the culture medium was measured using an LDH Cytotoxicity Assay Kit (Cayman Chemical Co, Ann Arbor, MI, USA) according to the manufacturer's instructions. The red formazan product was measured at 490 nm using a multiplate reader (VERSA max; Molecular Devices LLC, Sunnyvale, CA, USA). Positive control cells were cultured in medium containing 0.01% Triton X-100 and permeability was defined as 100%. Experiments were performed in triplicate.

### Assessment of CNT uptake by laser scanning confocal microscopy (LSM)

Cells were treated with CellLight® Lysosomes-RFP and Early Endosomes-GFP (Life Technologies) according to the manufacturer's instructions, and cultured on µ-Slide 8-well chambered slides with an ibiTreat surface (ibidi GmbH, Martinsried, Germany) for 24 hours in a 5% CO<sub>2</sub> incubator. After the cells were treated, they were incubated with or without CNTs (1 µg/mL in BEAS-2B and 10 µg/mL in MESO-1 cells) for 24 hours. Before observation, the cells were stained with bisbenzimidazole H333342 fluorochrome trihydrochloride ([H333342] 1 µg/mL) for 30 minutes. Cells were visualized with differential interference contrast optics and by fluorescence using an LSM510 NLO confocal microscope (Carl Zeiss Meditec AG, Jena, Germany) equipped with blue diode (360 nm), argon (488 nm), and helium–neon (543 nm) lasers for excitation of H333342, GFP, and RFP, respectively.

### Assessment of CNT uptake by transmission electron microscopy (TEM)

Cells grown on cover slips in a 3.5 cm culture dish were exposed to CNTs (1 µg/mL in BEAS-2B and 10 µg/mL in MESO-1 cells) for 24 hours. Cells were washed twice in PBS, fixed with 2.5% glutaraldehyde, postfixed with 1% osmic

acid, and embedded in Epon. Sections were cut at 60 nm, stained with uranyl acetate and lead citrate, and visualized under a JEM1400 transmission electron microscope (JEOL, Tokyo, Japan) at 80 keV.

### Total reactive oxygen species (ROS)/superoxide production

Total ROS/superoxide production in cells exposed to CNTs was determined using a total ROS/superoxide detection kit (Enzo Life Sciences, Inc., Farmingdale, NY, USA) according to the manufacturer's instructions. After the cells had adhered for 24 hours in 12-well plates, they were pretreated with oxidative stress detection reagent and superoxide detection reagent for 30 minutes before CNT solution (1 µg/mL in BEAS-2B and 10 µg/mL in MESO-1 cells) was added. Pyocyanin (100 µM) was used to induce ROS production. After 60 minutes, the cells were washed once with 1× wash buffer and harvested with trypsin–ethylenediaminetetraacetic acid. Cells were resuspended in 0.3 mL 1× wash buffer with 10% FBS and passed through a nylon mesh; then, they were subjected to flow cytometry (FACSCalibur™; BD Biosciences, San Jose, CA, USA) using the FL1 and FL2 channels for oxidative stress detection reagent and superoxide detection reagent signals, respectively, until 10,000 cells were recorded. Cell suspensions were assayed in triplicate for each treatment condition.

### Evaluation of intracellular acidity

To assess lysosomal acidity,<sup>36</sup> cells were adhered in a 12-well plate for 24 hours and exposed to CNTs (1 or 10 µg/mL in BEAS-2B and 1, 10, or 50 µg/mL in MESO-1 cells) for 24 hours. Cells were washed twice with PBS, and then incubated for 30 minutes under growth conditions in prewarmed medium containing 1 µM LysoSensor™ Green DND-189 dye (Life Technologies). After washing with PBS, cells were resuspended in PBS containing 10% FBS and subjected to flow cytometry until 10,000 cells were recorded. Cell suspensions were assayed in quadruplicate for each treatment condition and the LysoSensor intensity (%) was calculated. Since CNTs may interfere with the fluorescence signal during flow cytometry, control cells that were not exposed to CNTs prior to incubation with LysoSensor were prepared as a CNT blank, and CNTs were added before resuspension. CNT blank samples were assayed and the CNT inhibition intensity (%) was calculated. The change in % intensity was calculated as follows:

$$\Delta\% \text{ intensity} = \frac{\text{LysoSensor intensity} - \text{CNT inhibition intensity}}{\text{intensity}} \quad (2)$$

To obtain images of intracellular acidity levels, BEAS-2B cells treated with Lysosomes-RFP were adhered on  $\mu$ -Slide 8-well chambered slides for 24 hours and incubated with or without 1  $\mu$ g/mL CNT for 24 hours. Cells were washed twice with PBS, and then incubated for 30 minutes under growth conditions in prewarmed medium containing 1  $\mu$ M LysoSensor dye. Cells were visualized by fluorescence microscopy (Axio Observer.Z1; Carl Zeiss) using a 40 $\times$  objective.

### Statistical analysis

All data are presented as mean  $\pm$  standard error. Values were obtained from at least three independent experiments. The Student's *t*-test was used to compare means, and  $P < 0.05$  was considered statistically significant.

## Results

### CSCNTs have lower toxicity than MWCNTs

The cytotoxicity of CNTs was assessed using the AB assay (Figure 1A). The toxicity of MWCNTs in BEAS-2B

cells was concentration dependent, but did not vary as a function of length or diameter. The toxicity of CSCNTs in BEAS-2B cells was dependent on concentration and length (Figure 1B). In MESO-1 cells, MWCNT toxicity varied by concentration and was consistently lower than in BEAS-2B cells (Figure 1C). CSCNTs were not toxic to MESO-1 cells, except at the highest concentrations (50  $\mu$ g/mL) of CS-L and CS-M (Figure 1D). MWCNTs were more toxic than CSCNTs in both cell lines.

### BEAS-2B cells are more permeable to MWCNTs than CSCNTs

The LDH assay was used to evaluate plasma membrane permeability. BEAS-2B cells were more permeable to MWCNTs (>50%) than CSCNTs (<50%) at a CNT concentration of 10  $\mu$ g/mL (Figure 2A). Among MWCNTs, permeability to VGCF-X was highest at 77%, followed by VGCF-S and VGCF; for CSCNTs, permeability was CS-M  $\geq$  CS-L > CS-S. The permeability of MESO-1 cells to both types of CNT was <30%, with cells being most permeable

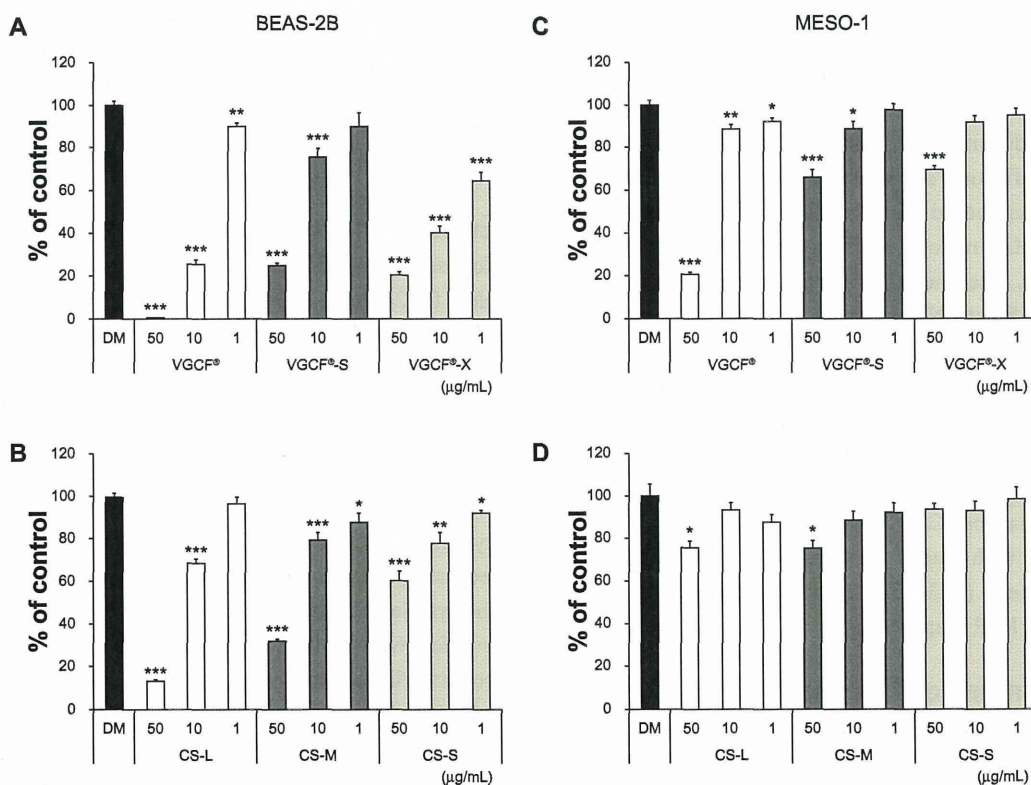


**Figure 1** Cell viability upon exposure to CNTs.

**Notes:** Cells were exposed to the indicated concentrations of CNT for 24 hours. BEAS-2B cells exposed to (A) MWCNTs (VGCF<sup>®</sup>-X, VGCF<sup>®</sup>-S, and VGCF<sup>®</sup>) and (B) CSCNTs (CS-L, CS-S, and CS-M). MESO-1 cells exposed to (C) MWCNTs and (D) CSCNTs. DM (0.001% gelatin) served as the control, and data are expressed as mean  $\pm$  standard error (n=6). \* $P < 0.05$ ; \*\* $P < 0.01$ ; \*\*\* $P < 0.001$ . MWCNTs were provided by Showa Denko KK (Tokyo, Japan); CSCNTs were provided by GSI Creos (Tokyo, Japan); VGCF, vapor grown carbon fibers; CS-L, CSCNT of length 20–80  $\mu$ m; CS-S, CSCNT of length 0.5–20  $\mu$ m; CS-M, CSCNT of intermediate length.

**Abbreviations:** CNT, carbon nanotube; CSCNT, cup-stacked CNT; DM, dispersant medium; MWCNT, multi-walled CNT; VGCF, vapor grown carbon fibers; CS-L, CSCNT of length 20–80  $\mu$ m; CS-S, CSCNT of length 0.5–20  $\mu$ m; CS-M, CSCNT of intermediate length.

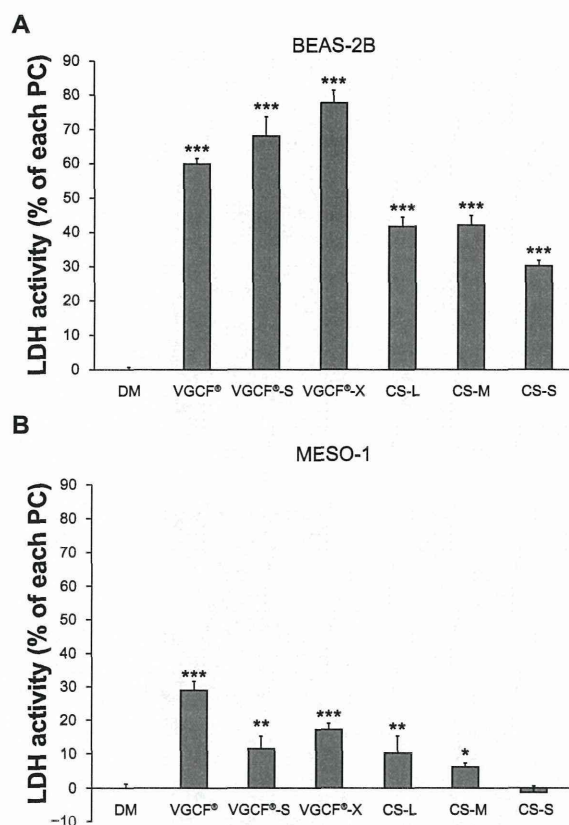


**Figure 2** Plasma membrane permeability in cells exposed to CNTs. **Notes:** Cells were exposed to 10  $\mu\text{g/mL}$  CNT for 24 hours. **(A)** BEAS-2B and **(B)** MESO-1 cells exposed to MWCNTs or CSCNTs. The LDH activity was calculated by the formula  $[(\text{experimental value} - \text{DM value})/(\text{PC value} - \text{DM value})] \times 10 \times 100$  (%). PC is 0.01% Triton X-100; DM is 0.001% gelatin. Data are compared to the control (DM) and expressed as mean  $\pm$  standard error ( $n=3$ ). \* $P<0.05$ ; \*\* $P<0.01$ ; \*\*\* $P<0.001$ . MWCNTs were provided by Showa Denko KK (Tokyo, Japan); CSCNTs were provided by GSI Creos (Tokyo, Japan). **Abbreviations:** CNT, carbon nanotube; CSCNT, cup-stacked CNT; DM, dispersant medium; LDH, lactate dehydrogenase; MWCNT, multi-walled CNT; PC, positive control; VGCF, vapor grown carbon fibers; CS-L, CSCNT of length 20–80  $\mu\text{m}$ ; CS-S, CSCNT of length 0.5–20  $\mu\text{m}$ ; CS-M, CSCNT of intermediate length.

to VGCF at 29% (Figure 2B). In general, permeability followed a trend that was similar, but not identical, to cytotoxicity in both cell types, with membrane permeability at 10  $\mu\text{g/mL}$  reflecting the trend for cytotoxicity at 50  $\mu\text{g/mL}$ .

### MWCNTs and CSCNTs aggregate in the lysosome of BEAS-2B cells

BEAS-2B cells that had endocytosed CNTs were observed by LSM and TEM (Figures 3A and 4A). Cells were treated with fluorescent protein-signal peptide fusion molecules to visualize the lysosome (RFP) and early endosome (GFP). GCF, VGCF-S, and CS-L were visible as multiple long fiber bundles adjacent to the nucleus and were seen protruding from the lysosome (Figure 3Ab, 3Ac, and 3Ae). Although a similar distribution of

the fibers was observed with VGCF-X and CS-S, for the former, only a portion of the agglomerate was inside the lysosome while the majority of fibers penetrated the plasma membrane, as opposed to CS-S fibers, which were mostly in the lysosomal compartment (Figure 3Ad and 3Ag). CS-Ms were observed as both single fibers and aggregates and appeared as a mixture of CS-Ls and CS-Ss (Figure 3Af). There was no overlap in the signals of early endosomes and CNTs in the cytoplasm of BEAS-2B and MESO-1 cells. The lysosomal distribution of VGCF, VGCF-S, and CS-L was more clearly visible by TEM (Figure 4Ab, 4Ac and 4Ae). Two pits were observed in the process of endocytosis of VGCF-X aggregates (Figure 4Ag).

Although MESO-1 cells were exposed to MWCNTs and CSCNTs at a tenfold higher concentration than BEAS-2B cells (Figure 3B), CNT fibers and agglomerates were not specifically associated with the lysosome and were instead distributed throughout the cytoplasm while being excluded from the nucleus, with no obvious effects on adhesion or viability. In TEM images, a few isolated VGCF and VGCF-S fibers were observed adjacent to nuclei (Figure 4Bb and 4Bc), while the other CNTs were present as aggregates (Figure 4Bd–g).

### MWCNTs stimulate ROS production in BEAS-2B cells

The total ROS production in BEAS-2B cells exposed to MWCNTs and CSCNTs is shown in Figure 5A. Oxidative stress was significantly upregulated, and superoxide dismutase activity was slightly increased by VGCF-X compared to that for the positive control pyocyanin. An increase in oxidative stress level was observed in MESO-1 cells exposed to VGCF-X (Figure 5B).

### CNTs induce lysosomal acidification upon uptake

An acidotropic probe, which accumulates in acidic organelles and exhibits pH-dependent increases in fluorescence intensity upon acidification, was used to evaluate changes in intracellular acidity upon exposure to CNTs. Cells that had internalized CNTs were isolated by flow cytometry (Figure 6A and B). BEAS-2B cells exposed to 50  $\mu\text{g/mL}$  MWCNTs were not analyzed because a sufficient number of living cells could not be obtained for analysis due to the toxicity of MWCNTs at this concentration. Increases in intensity upon exposure of BEAS-2B cells to 1  $\mu\text{g/mL}$  VGCF, VGCF-S, and VGCF-X were 10.8%, 7.5%, and 17.5%, respectively, while, for CSCNTs at the same concentration, the values were <5% (Figure 6A). However, at 10  $\mu\text{g/mL}$ , all CNTs induced increases in intensity of >10% in BEAS-2B cells.

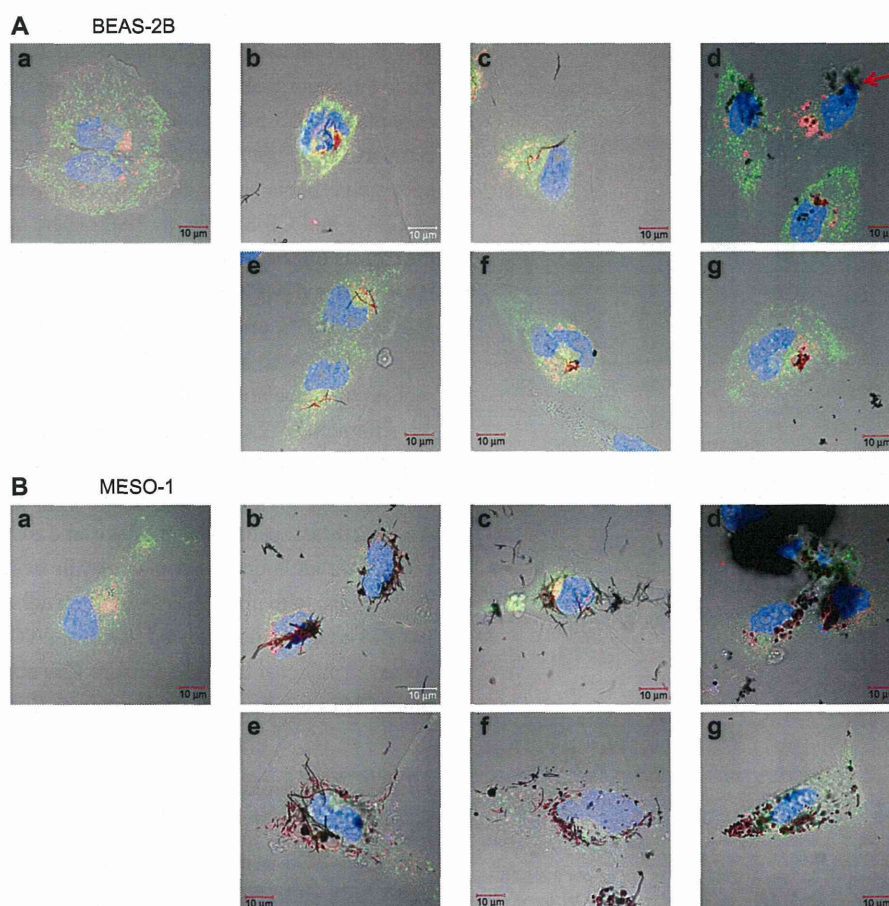


**Figure 3** Live cells imaged by differential interference contrast optics after incubation with CellLight® Lysosomes-RFP and Early Endosomes-GFP (Life Technologies, Carlsbad, CA, USA) and bisbenzimidazole H333342 fluorochrome trihydrochloride for nuclear staining.

**Notes:** (A) BEAS-2B cells were exposed to 1  $\mu\text{g}/\text{mL}$  MWCNT (VGCF) or CSCNT (CS) for 24 hours. (a) DM (control); (b) VGCF<sup>®</sup>; (c) VGCF<sup>®</sup>-S; (d) VGCF<sup>®</sup>-X; (e) CS-L; (f) CS-M; and (g) CS-S. Red arrow indicates VGCF-X agglomerates, which were not taken up by BEAS-2B cells, nor did they fully penetrate the cell membrane. Scale bar = 10  $\mu\text{m}$ . (B) MESO-1 cells were exposed to 10  $\mu\text{g}/\text{mL}$  MWCNT (VGCF) or CSCNT (CS) for 24 hours. (a) DM (control); (b) VGCF; (c) VGCF-S; (d) VGCF-X; (e) CS-L; (f) CS-M; and (g) CS-S. Scale bar = 10  $\mu\text{m}$ . MWCNTs were provided by Showa Denko KK (Tokyo, Japan); CSCNTs were provided by GSI Creos (Tokyo, Japan).

**Abbreviations:** CSCNT, cup-stacked carbon nanotube; DM, dispersant medium; MWCNT, multi-walled carbon nanotube; CS-L, CSCNT of length 20–80  $\mu\text{m}$ ; CS-S, CSCNT of length 0.5–20  $\mu\text{m}$ ; CS-M, CSCNT of intermediate length.

In contrast, in MESO-1 cells, changes were mostly  $\leq 10\%$ , with VGCF and VGCF-S (at 50  $\mu\text{g}/\text{mL}$ ) accounting for more than 30% of the total increase (Figure 6B). To determine whether acidification was due to CNT uptake, the lysosomes of BEAS-2B cells exposed to 10  $\mu\text{g}/\text{mL}$  CNT and treated with the acidotropic probe were visualized, while control cells were double-stained with Lysosomes-RFP dye and emitted orange fluorescence (Figure 6C). Small vacuoles were observed in CNT-exposed cells, but CNT aggregates were visible only in lysosomes, confirming that the observed increases in intensity were due to lysosomal CNT uptake.

## Discussion

A major concern for the use of CNTs is their safety, since their shape is similar to that of asbestos. Although CNTs need

to be internalized by cells in order to be useful as carriers, intracellular accumulation can be cytotoxic.<sup>32</sup> A number of studies have investigated the biodegradability of CNTs in an attempt to address this issue.<sup>37–39</sup> However, CNTs are inherently stable, and degradation by chemical modification has yet to be developed. Therefore, the present study examined the optimal CNT shape and size that can maximize biocompatibility using two different types of CNT.

Both BEAS-2B and MESO-1 cells internalized MWCNTs, but different cytotoxic effects were observed in each cell line. In BEAS-2B cells, toxicity varied as a function of diameter, such that the toxicity was VGCF > VGCF-X > VGCF-S, while for MESO-1 cells, the order was VGCF > VGCF-S  $\geq$  VGCF-X (Figure 1). In another study, macrophages, but not mesothelial or



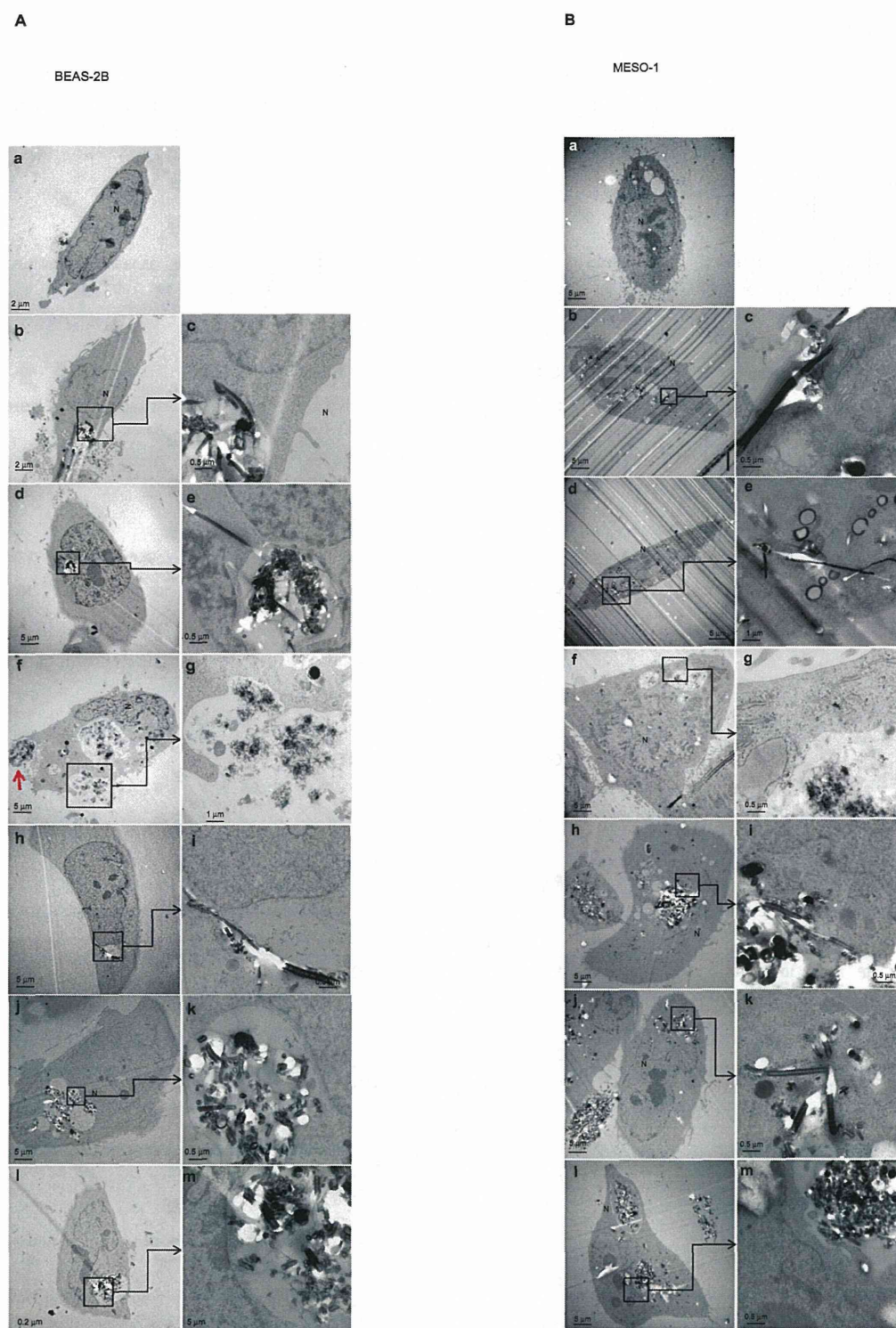
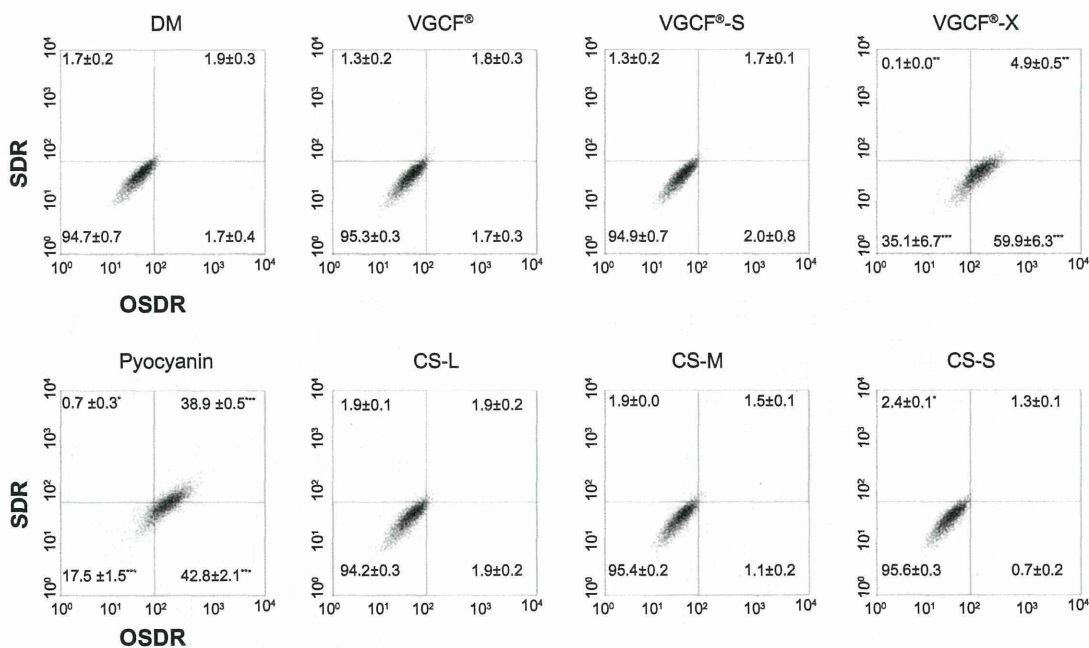


**Figure 4** Transmission electron micrographs of BEAS-2B and MESO-1 cells exposed to CNTs.

**Notes:** (A) BEAS-2B cells were exposed to 1  $\mu\text{g}/\text{mL}$  MWCNT (VGCF) or CSCNT (CS) for 24 hours. (a) DM (control); (b and c) VGCF<sup>®</sup>; (d and e) VGCF<sup>®</sup>-S; (f and g) VGCF<sup>®</sup>-X; (h and i) CS-L; (j and k) CS-M; and (l and m) CS-S. Red arrow indicates VGCF-X agglomerates, which were not taken up by BEAS-2B cells, nor did they fully penetrate the cell membrane. (B) MESO-1 cells were exposed to 10  $\mu\text{g}/\text{mL}$  MWCNT or CSCNT for 24 hours. (a) DM (control); (b and c) VGCF; (d and e) VGCF-S; (f and g) VGCF-X; (h and i) CS-L; (j and k) CS-M; and (l and m) CS-S. MWCNTs were provided by Showa Denko KK (Tokyo, Japan); CSCNTs were provided by GSI Creos (Tokyo, Japan).

**Abbreviations:** CNT, carbon nanotube; CSCNT, cup-stacked carbon nanotube; DM, dispersant medium; MWCNT, multi-walled carbon nanotube; CS-L, CSCNT of length 20–80  $\mu\text{m}$ ; CS-S, CSCNT of length 0.5–20  $\mu\text{m}$ ; CS-M, CSCNT of intermediate length; VGCF, vapor grown carbon fibers.

**A BEAS-2B**



**B MESO-1**

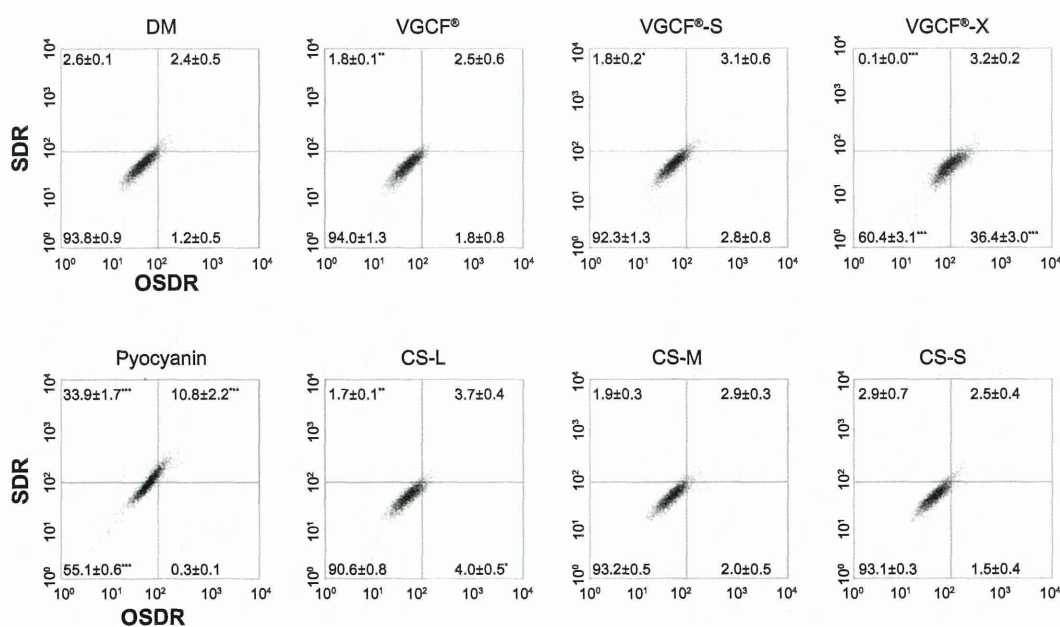


**Figure 5** Total reactive oxygen species production upon exposure to CNTs.

**Notes:** (A) BEAS-2B cells were exposed to 1 µg/mL MWCNT (VGCF<sup>®</sup>, VGCF<sup>®</sup>-S, and VGCF<sup>®</sup>-X) or CSCNT (CS-L, CS-M, and CS-S) for 1 hour. (B) MESO-1 cells were exposed to 10 µg/mL MWCNT (VGCF, VGCF-S, and VGCF-X) or CSCNT (CS-L, CS-M, and CS-S) for 1 hour. Pyocyanin (100 µM) was used to induce the production of reactive oxygen species. Data are expressed as mean ± standard error (n=3). \*P<0.05; \*\*P<0.01; \*\*\*P<0.001. MWCNTs were provided by Showa Denko KK (Tokyo, Japan); CSCNTs were provided by GSI Creos (Tokyo, Japan).

**Abbreviations:** CNT, carbon nanotube; CSCNT, cup-stacked carbon nanotube; DM, dispersant medium; MWCNT, multi-walled carbon nanotube; OSDR, oxidative stress detection reagent; SDR, superoxide detection reagent; CS-L, CSCNT of length 20–80 µm; CS-S, CSCNT of length 0.5–20 µm; CS-M, CSCNT of intermediate length; VGCF, vapor grown carbon fibers.